LETTER

doi:10.1038/nature12348

Activity-dependent phosphorylation of MeCP2 threonine 308 regulates interaction with NCoR

Daniel H. Ebert[1,2], Harrison W. Gabel[1], Nathaniel D. Robinson[1], Nathaniel R. Kastan[1], Linda S. Hu[1], Sonia Cohen[1], Adrija J. Navarro[1], Matthew J. Lyst[3], Robert Ekiert[3], Adrian P. Bird[3] & Michael E. Greenberg[1]

Rett syndrome (RTT) is an X-linked human neurodevelopmental disorder with features of autism and severe neurological dysfunction in females. RTT is caused by mutations in methyl-CpG-binding protein 2 (MeCP2), a nuclear protein that, in neurons, regulates transcription, is expressed at high levels similar to that of histones, and binds to methylated cytosines broadly across the genome[1–5]. By phosphotryptic mapping, we identify three sites (S86, S274 and T308) of activity-dependent MeCP2 phosphorylation. Phosphorylation of these sites is differentially induced by neuronal activity, brain-derived neurotrophic factor, or agents that elevate the intracellular level of 3′,5′-cyclic AMP (cAMP), indicating that MeCP2 may function as an epigenetic regulator of gene expression that integrates diverse signals from the environment. Here we show that the phosphorylation of T308 blocks the interaction of the repressor domain of MeCP2 with the nuclear receptor co-repressor (NCoR) complex and suppresses the ability of MeCP2 to repress transcription. In knock-in mice bearing the common human RTT missense mutation R306C, neuronal activity fails to induce MeCP2 T308 phosphorylation, suggesting that the loss of T308 phosphorylation might contribute to RTT. Consistent with this possibility, the mutation of MeCP2 T308A in mice leads to a decrease in the induction of a subset of activity-regulated genes and to RTT-like symptoms. These findings indicate that the activity-dependent phosphorylation of MeCP2 at T308 regulates the interaction of MeCP2 with the NCoR complex, and that RTT in humans may be due, in part, to the loss of activity-dependent MeCP2 T308 phosphorylation and a disruption of the phosphorylation-regulated interaction of MeCP2 with the NCoR complex.

The location of RTT missense mutations provides insight into MeCP2's function. Of the four most common RTT missense mutations, three—at R106, R133 and T158—are in the DNA-binding domain and disrupt binding to methylated DNA, suggesting that binding to methylated DNA is critical for MeCP2 function[6–8]. Disruption of binding to methylated DNA probably impairs MeCP2's function as a repressor. Consistent with this possibility, the fourth common RTT missense mutation, R306C, is located within the repressor domain of MeCP2. However, the mechanism of action of the MeCP2 repressor domain and the specific functions of R306 were not known.

Recent evidence indicates that sensory stimulation triggers MeCP2 phosphorylation at a specific site, S421, raising the possibility that MeCP2 may function as a neuronal activity-regulated repressor, and that RTT may result from the de-regulation of neuronal activity-dependent gene programs[9–13]. However, studies of knock-in mice in which S421 is converted to an alanine have challenged this hypothesis, as this mutation had no detectable effect on gene transcription[14].

To search for additional activity-dependent sites of MeCP2 phosphorylation that might regulate MeCP2 function, we performed phosphotryptic mapping of MeCP2 derived from ^{32}P-orthophosphate-labelled neurons that were left untreated or exposed to elevated levels of KCl to trigger membrane depolarization and calcium influx. Lysates from these neurons were incubated with anti-MeCP2 antibodies, and immunoprecipitates were resolved by SDS–PAGE. The band corresponding to MeCP2 was excised and digested with trypsin. Phosphopeptides were resolved by two-dimensional thin-layer electrophoresis and chromatography. Autoradiography of the phosphotryptic maps revealed a complex pattern of MeCP2 phosphorylation in both untreated and membrane-depolarized neurons, indicating that MeCP2 is phosphorylated at many sites in cultured neurons (Fig. 1a). However, three phosphopeptides, indicated as *a*, *b* and *c* in Fig. 1a, appeared reproducibly after membrane depolarization. The same inducible phosphopeptides were detected in MeCP2 S421A knock-in neurons, indicating that these phosphopeptides do not contain S421.

To identify the site(s) of inducible MeCP2 phosphorylation, we compared phosphotryptic maps of MeCP2 phosphorylated *in vitro* by calcium-regulated kinases with the phosphotryptic maps of MeCP2 obtained from membrane-depolarized neurons. Once a kinase was identified that phosphorylated MeCP2 *in vitro* at a site that co-migrated with spots *a*, *b*, or *c* on the phosphotryptic map from primary neuronal culture, we mutated MeCP2 to identify the candidate sites of phosphorylation. To characterize further these sites of MeCP2 phosphorylation, we generated phosphorylation site-specific antibodies to each of the sites. This analysis (Fig. 1 and Supplementary Figs 1–6) revealed that upon membrane depolarization, or upon stimulation with the $GABA_A$ (γ-aminobutyric acid subtype A)-receptor antagonist bicuculline, which relieves inhibitory input and allows for the release of endogenous glutamate in the cultures, MeCP2 becomes newly phosphorylated at S86, S274, T308 and S421. We note that S86 and T308 phosphorylation was not detected by previous mass spectrometry studies, underscoring the value of using phosphotryptic mapping to discover sites of activity-dependent phosphorylation in neurons.

To investigate whether phosphorylation of these sites on MeCP2 is inducible *in vivo*, mice were treated with kainic acid to trigger seizures and robust neuronal activity. Forebrain lysates from untreated and kainic-acid-injected mice were analysed by western blotting. We found that exposure to kainic acid reproducibly induced MeCP2 phosphorylation at S86, S274, T308 and S421 (Fig. 1b). In brain lysates from mice not exposed to kainic acid, a low level of immune reactivity is detected, suggesting that basal activity in the brain also induces phosphorylation of MeCP2 at each of these sites. These findings demonstrate that phosphorylation at MeCP2 S86, S274, T308 and S421 is induced by neuronal activity, both in cell culture and in the intact brain.

We next compared the ability of different extracellular stimuli to induce the phosphorylation of MeCP2. Cortical neurons were stimulated with KCl to induce membrane depolarization, with brain-derived neurotrophic factor (BDNF), or with forskolin to activate protein kinase A (PKA) (Fig. 1d). Western blotting of lysates of these stimulated cultures revealed that MeCP2 phosphorylation at S86 and S274 is induced significantly by either BDNF or forskolin and less well upon membrane depolarization with KCl. By contrast, MeCP2 phosphorylation at T308 and S421 is induced most effectively by membrane

[1]Department of Neurobiology, Harvard Medical School, Boston, Massachusetts 02115, USA. [2]Department of Psychiatry, Massachusetts General Hospital, Harvard Medical School, Boston, Massachusetts 02114, USA. [3]Wellcome Trust Centre for Cell Biology, University of Edinburgh, Edinburgh EH9 3JR, UK.

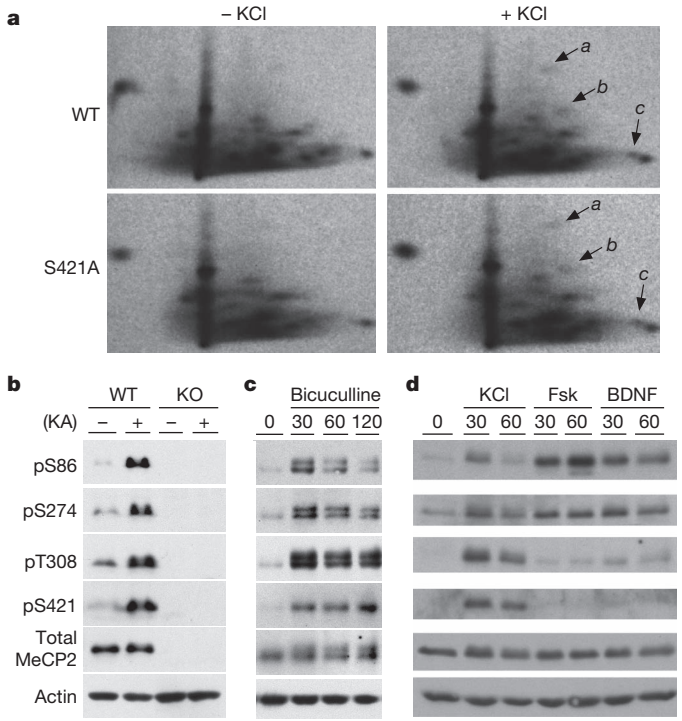

Figure 1 | Phosphotryptic mapping of MeCP2 identifies activity-dependent phosphorylation sites. **a**, Dissociated cortical cultures, derived from wild-type (WT) or MeCP2 S421A knock-in mice, were metabolically labelled with ^{32}P-orthophosphate and were left untreated or membrane depolarized with KCl. Phospho-peptides were spotted in the lower left corner of the plate, resolved by thin-layer electrophoresis in the horizontal direction and thin-layer chromatography in the vertical direction. The activity-induced spots are indicated (arrows *a*–*c*). **b**, Mice were injected with kainic acid (KA) to induce seizures. **c**, Cortical neurons were stimulated with bicuculline. **d**, Cortical neurons were membrane depolarized with KCl or treated with BDNF or forskolin (Fsk). Time of stimulation (min) is indicated. Lysates were examined by western blotting with the indicated antibodies. Phospho-site-specific antibodies are indicated by 'p' followed by the site. Findings were confirmed with at least three biological replicates from dissections of independent animals.

depolarization and less potently by BDNF or forskolin. These findings indicate that MeCP2 may be a convergence point in the nucleus for multiple signalling pathways and raise the possibility that differential phosphorylation of MeCP2, bound broadly across the genome, could mediate the response of neuronal chromatin to diverse stimuli. In a manner similar to the epigenetic regulation of gene expression by modifications of histones, the multiple stimulus-regulated post-translational modifications of MeCP2 may be a mechanism that modulates chromatin remodelling in post-mitotic neurons.

To assess the importance of phosphorylation at these novel sites for neuronal function and RTT, we focused our attention on the phosphorylation of MeCP2 T308 because of its proximity to common RTT missense mutations R306C/H. A possible clue to the function of phosphorylation of MeCP2 T308 was provided by a recent study demonstrating that the R306C mutation disrupts the ability of MeCP2 to interact with the NCoR complex[8]. NCoR forms a complex with multiple proteins, including histone deacetylase 3 (HDAC3), and this complex is thought to trigger histone deacetylation and gene repression[15–17]. Given the proximity of T308 to amino acids that are essential for recruitment of the NCoR complex, we postulated that phosphorylation of MeCP2 at T308 might affect the interaction of MeCP2 with the NCoR complex and might thereby mediate activity-dependent changes in gene expression.

We developed a peptide pull-down assay to examine the interaction of the repressor domain of MeCP2 with the NCoR complex and assessed the effect of MeCP2 T308 phosphorylation on this interaction (Fig. 2a, b and Supplementary Figs 7–9). We synthesized biotin-conjugated MeCP2-derived peptides in which T308 was either left unphosphorylated (np peptide) or phosphorylated at T308 (pT308 peptide), mixed the peptides with streptavidin-conjugated magnetic beads, and, by western blotting with various antibodies to components of the NCoR complex, assessed the ability of the beads to pull down the NCoR complex from brain lysates. The np peptide was able to pull down core components of the NCoR complex including HDAC3, TBL1, TBLR1 and GPS2, but not another co-repressor SIN3A, indicating that the region of MeCP2 surrounding T308 contains a binding site that specifically mediates the interaction of MeCP2 with the NCoR complex. By contrast, the pT308 peptide did not interact at all with the NCoR complex. Similarly, peptides containing phosphomimetic T308D and T308E mutations, acidic amino acid mutations that partially mimic a phosphorylated residue, showed reduced binding to the NCoR complex. The peptide pull-down experiments demonstrate that the carboxy-terminal region of MeCP2's transcription repression domain interacts with the NCoR complex and that phosphorylation of T308 abrogates this interaction. These findings suggest that neuronal-activity-induced phosphorylation of MeCP2 T308 disrupts the interaction of the repressor domain of MeCP2 with the NCoR complex and raise the possibility that, by altering the interaction of NCoR with MeCP2, the phosphorylation of T308 might affect MeCP2-dependent transcription. However, it remains to be determined whether the phosphorylation of MeCP2 T308 leads to a complete release of the NCoR complex from MeCP2 bound to methylated DNA, or if T308 phosphorylation disrupts the interaction of the MeCP2 repressor domain with NCoR without leading to a release of the NCoR complex.

To determine if MeCP2 T308 phosphorylation affects MeCP2's function as a transcriptional repressor, we assessed the ability of wild-type and mutant versions of MeCP2 (R306C, T308A, T308D and T308E) to repress reporter gene transcription (Fig. 2c and Supplementary Figs 8 and 9). Cultured cortical neurons were co-transfected with plasmid constructs expressing MeCP2 variants fused to the GAL4 DNA-binding domain (GAL4–MeCP2) and a firefly luciferase reporter plasmid with a promoter containing GAL4-binding sites (luciferase reporter)[8]. Upon transfection into cortical neurons together with the luciferase reporter, wild-type GAL4–MeCP2 effectively represses reporter gene transcription. However, insertion of the R306 to cysteine

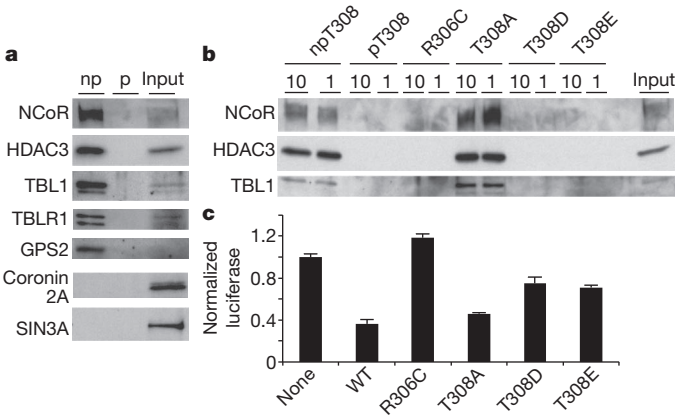

Figure 2 | Phosphorylation of T308 regulates MeCP2's interaction with the NCoR complex. **a**, Peptides corresponding to MeCP2, either not phosphorylated (np) or synthesized to be phosphorylated at the amino acid residue corresponding to 308 (p), were incubated with cortical neuron lysates. Pull downs were visualized by western blotting with the indicated antibodies. **b**, Peptide pull downs using synthetic peptides (at 10× or 1× concentration) containing one of the following mutations: R306C, T308A, T308D, or T308E. **c**, Luciferase reporter gene assay with plasmids encoding reporter and GAL4–MeCP2 variants, as indicated, transfected into cortical neurons. 'None' had no GAL4–MeCP2 variant transfected. Shown are averages and s.e.m. of three biological replicates. Findings for each experiment were confirmed with at least three biological replicates from dissections of independent litters.

mutation into GAL4–MeCP2 resulted in a version of GAL4–MeCP2 that is no longer capable of repressing transcription. Given that the mutation of MeCP2 R306 to C renders MeCP2 incapable of binding the NCoR complex, these findings suggest that GAL4–MeCP2 represses the GAL4 reporter gene in an NCoR-dependent manner. If the phosphorylation of MeCP2 at T308 blocks the ability of MeCP2 to repress transcription via the NCoR complex, we would expect that mutation of T308 to an acidic amino acid (D or E), which partially abolishes the interaction of MeCP2 with the NCoR complex, should partially suppress GAL4–MeCP2-dependent transcription repression. This is what we observed when GAL4–MeCP2 T308D or GAL4–MeCP2 T308E were tested for their ability to repress reporter gene transcription. The intermediate loss of the transcription repression by the GAL4–MeCP2 T308D/E variants corresponds with partial loss of binding to the NCoR complex that we observed by western blotting (Supplementary Fig. 9). By contrast, GAL–MeCP2 T308A, a mutant MeCP2 that is still capable of interacting with the NCoR complex, was fully capable of repressing luciferase reporter gene transcription. These findings suggest that phosphorylation of MeCP2 T308 prevents the interaction of the repressor domain of MeCP2 with the NCoR complex, thereby reducing MeCP2–NCoR–HDAC3-mediated transcriptional repression.

We next asked if the activity-dependent phosphorylation of MeCP2 T308 affects the ability of MeCP2 to function as a repressor of activity-dependent gene transcription. Towards this end we generated mice in which MeCP2 T308 is converted to an alanine (MeCP2 T308A knock-in mice) and assessed the effect of this mutation on activity-dependent gene transcription. We first demonstrated by western blotting that MeCP2 T308A knock-in mice and their wild-type littermates express equivalent levels of MeCP2 protein (Supplementary Fig. 10a, b). This indicates that the T308A mutation does not alter the stability of MeCP2. In addition, we confirmed by western blotting with anti-MeCP2 phospho-T308 antibodies that the MeCP2 T308A knock-in neurons lack T308 phosphorylation (Supplementary Fig. 10c). We also demonstrated by chromatin immunoprecipitation with anti-MeCP2 antibodies that the T308A mutation does not affect MeCP2 binding to DNA (Supplementary Fig. 10d), and by peptide pull-down experiments (Fig. 2b) and co-immunoprecipitation of MeCP2 and NCoR from forebrain extracts (Supplementary Fig. 10e) that the T308A mutation does not disrupt the basal binding of MeCP2 to the NCoR complex. These findings suggest that any abnormality that we detect in gene transcription in MeCP2 T308A knock-in mice might be attributed to the loss of the phosphorylation-dependence of the interaction of MeCP2 with the NCoR complex rather than to a decrease in MeCP2's expression, binding to DNA, or ability to interact with NCoR.

We assessed the effect of the MeCP2 T308A mutation on activity-dependent gene transcription directly by exposing cultured neurons derived from wild-type and MeCP2 T308A knock-in mice to elevated levels of KCl and monitoring activity-dependent gene expression by PCR with reverse transcription (RT–PCR) (Fig. 3a). We found that membrane depolarization induces *Arc*, *Fos*, *Nptx2* and *Adcyap1* messenger RNA expression equivalently in wild-type and MeCP2 T308A knock-in neurons, indicating that the signalling apparatus that conveys the membrane depolarization/calcium signal to the nucleus to activate gene transcription functions normally in MeCP2 T308A knock-in neurons. By contrast, membrane depolarization induces significantly less *Npas4* in MeCP2 T308A knock-in neurons than in wild-type neurons. Previous studies have shown that *Npas4* expression is induced upon membrane depolarization of excitatory neurons and that NPAS4 promotes the development of inhibitory synapses on excitatory neurons[18], a process that has been found to be abnormal in RTT[19]. NPAS4 is a transcription factor that has been suggested to regulate inhibitory synapse number by activating expression of *Bdnf* (ref. 18). Therefore, we investigated whether *Bdnf* might also be impaired in T308A knock-in neurons compared to wild-type neurons. There is a trend towards decreased induction of *Bdnf* mRNA in T308A knock-in neurons compared to wild-type neurons. We also observed an attenuation of light induction of *Npas4* and *Bdnf* in the visual cortex of dark-reared T308A knock-in compared to wild-type mice but no statistically significant difference in *Arc*, *Fos*, *Nptx2* and *Adcyap1* mRNA transcription in these two strains of mice (Fig. 3b). This suggests that the decrease in activity-dependent *Npas4* and *Bdnf* expression in T308A knock-in compared to wild-type mice occurs *in vivo* and could, in principle, contribute to neural circuit defects that occur in RTT. These findings are consistent with a model in which activity-dependent phosphorylation of MeCP2 T308 leads to a decrease in the association of the NCoR co-repressor complex with the repressor domain of MeCP2, thus facilitating activity-dependent *Npas4* transcription and the subsequent activation of *Bdnf* transcription. However, given that MeCP2 binds broadly across the genome, we cannot rule out the possibility that, in MeCP2 T308A knock-in mice, the reduction in neuronal activity-dependent induction of *Npas4* and *Bdnf* mRNA is due to an effect of the T308A mutation on chromatin architecture that affects excitatory/inhibitory balance and only indirectly leads to a reduction in the levels of *Npas4* and *Bdnf* mRNA.

Finally, we sought to determine if the disruption of activity-dependent phosphorylation of MeCP2 T308 and the consequent disruption of activity-dependent gene transcription contributes to RTT. We first noted that T308 is in close proximity to common RTT missense mutations at R306C/H. Given that the kinases that can phosphorylate T308 (CaMKIV and PKA) typically require a basophilic residue two or three amino acids amino-terminal to the site of phosphorylation[20], we hypothesized that R306C/H mutations, in addition to abolishing the interaction of MeCP2 with the NCoR complex, might render MeCP2 refractory to phosphorylation at T308. To test this hypothesis, we

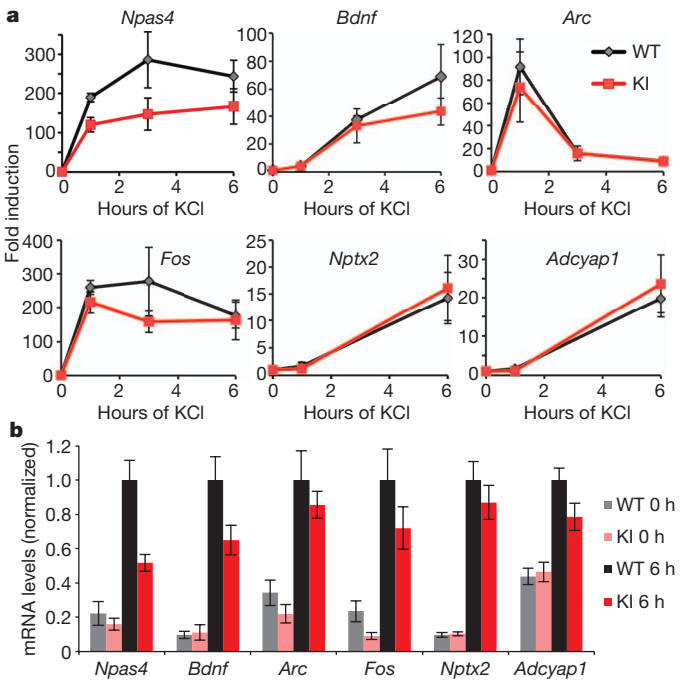

Figure 3 | MeCP2 T308A knock-in mice have altered activity-dependent gene expression. **a**, Dissociated cortical neuron cultures, generated from MeCP2 T308A knock-in mice (KI, red) and wild-type littermates (WT, black), were membrane depolarized with KCl. Shown are fold-inductions of RT–PCR values for the average of three independent days of dissection (biological replicates). For *Npas4*, *P* values were 0.024 (repeated measures ANOVA) and 0.03 at 1 h and 0.01 at 6 h (paired two-tailed *t*-test). **b**, Eight-week-old mice, kept in the dark for the previous 2 weeks, were either kept in the dark (0 h) or exposed to a light source for 6 h (6 h). From dissected visual cortices, RT–PCR values were divided by the average of WT 6 h. The numbers of littermate mice averaged per time point were: WT 0 h ($n = 6$), KI 0 h ($n = 6$), WT 6 h ($n = 8$) and KI 6 h ($n = 10$). Error bars indicate s.e.m. For *Npas4* at 6 h, the two-tailed *t*-test *P* value is 0.0007 and for *Bdnf* at 6 h, the *P* value is 0.04.

exposed wild-type or MeCP2 R306C knock-in mice[8] to kainic acid, prepared lysates from hippocampi, and assessed the phosphorylation of MeCP2 at T308 by western blotting (Fig. 4a). Exposure of mice to kainic acid induced the phosphorylation of MeCP2 T308 in wild-type but not MeCP2 R306C knock-in mice despite equivalent expression of total MeCP2 in both genotypes. Notably, we confirmed that the anti-MeCP2 pT308 antibodies are still able to recognize phosphorylated-T308 in the presence of the R306C mutation (Supplementary Fig. 11). Taken together, these findings indicate that the common R306C/H mutations that occur in RTT not only disrupt the interaction of MeCP2 with the NCoR, they also abrogate activity-dependent phosphorylation of MeCP2 at T308. Thus, RTT in individuals with R306C/H mutations could result simply from the loss of basal NCoR binding to MeCP2, which, by necessity, would abolish the regulated interaction of MeCP2 with NCoR. However, it is possible that the loss of activity-dependent MeCP2 T308 phosphorylation could, in and of itself, contribute to aspects of RTT in these individuals. It is also possible that the loss of MeCP2 T308 phosphorylation could have consequences, in addition to the disruption of the proper regulation of NCoR binding, which may also be relevant to the aetiology of RTT.

To investigate whether activity-dependent MeCP2 T308 phosphorylation might contribute to RTT, we asked if MeCP2 T308A knock-in mice display neurological impairments that are hallmarks of RTT, including reduced brain weight, motor abnormalities, and a reduced threshold for the onset of seizures (Fig. 4b–e and Supplementary Fig. 12). As discussed above, MeCP2 T308A knock-in mice, when compared to wild-type littermates, have normal levels of MeCP2 protein expression, binding to DNA, and interaction with the NCoR complex. These findings suggest that any neurological phenotypes observed in the MeCP2 T308A knock-in mice are most probably due to the disruption of T308 phosphorylation and the loss of the phosphorylation-dependence of the interaction of MeCP2 with the NCoR complex. The first indication that MeCP2 T308A knock-in mice have neurological deficits was that the brains of MeCP2 T308A knock-in mice weigh significantly less than the brains of their wild-type littermates despite the fact that the overall body weights of these two types of mice are similar (Fig. 4b). We also found that when compared to wild-type littermate controls, MeCP2 T308A knock-in mice display hindlimb clasping and a reduced ability to stay on an accelerating rotarod, two phenotypes that indicate that MeCP2 T308A knock-in mice have motor system defects (Fig. 4c, d). To determine whether MeCP2 T308A knock-in mice have a lower seizure threshold, wild-type and MeCP2 T308A knock-in mice were exposed to a low-dose of the GABA antagonist pentylenetetrazol (PTZ), and the time to onset and frequency of generalized tonic-clonic seizures measured (Fig. 4e). Compared to wild-type littermates, the MeCP2 T308A knock-in mice have more seizures, and the onset of the seizures occurs more rapidly. These findings suggest that the MeCP2 T308A knock-in mice have a lower seizure threshold compared to wild-type mice. This decrease in seizure threshold could be due to the decrease in *Npas4* and *Bdnf* transcription in MeCP2 T308A knock-in mice and the consequent disruption of excitatory/inhibitory balance in the brains of these animals[18,21]. Although a direct comparison has not yet been performed, the MeCP2 R306C knock-in mice clearly have a more severe phenotype than the MeCP2 T308A knock-in mice[8], consistent with the R306C mutation abolishing the binding to the NCoR complex and the T308A mutation disrupting the activity-regulated interaction with the NCoR complex. Taken together, these findings indicate that the loss of activity-regulated phosphorylation of T308, and the disruption of activity-dependent control of the interaction of MeCP2 with the NCoR complex, probably contribute to some of the neurological deficits in RTT.

How could loss of NCoR binding (MeCP2 R306C mice[8]) and constitutive NCoR binding (MeCP2 T308A mice) both lead to a RTT-like syndrome? A possible answer may come from previous studies demonstrating that both loss of MeCP2 and overexpression of MeCP2 can lead to RTT-like symptoms, although of varying severity[22,23]. The R306C phenotype may be analogous to MeCP2 loss of function RTT (MeCP2 can no longer bind NCoR), whereas the T308A phenotype may be similar to MeCP2 gain-of-function phenotype (MeCP2 constitutively binds NCoR and is a constitutively active repressor). Taken together, the MeCP2 R306C and MeCP2 T308A knock-in studies provide evidence that the interaction of MeCP2 with the NCoR complex is critical for proper MeCP2 function, and that dysregulation of this interaction can lead to RTT.

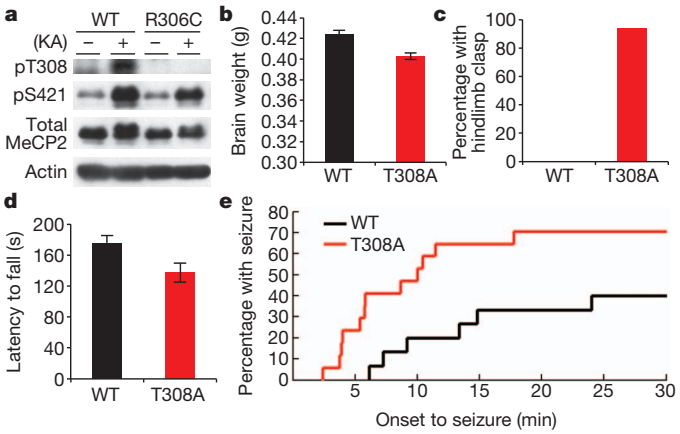

Figure 4 | Phosphorylation of MeCP2 T308 is a key mechanism underlying RTT. a, MeCP2 R306C knock-in mice and wild-type littermates (WT) were treated with kainic acid (KA) to induce seizures or left untreated (−). Forebrain lysates were resolved by western blot analysis with indicated antibodies. Findings were confirmed with five biological replicates from independent animals. **b**, Brains were dissected and weighed for T308A knock-in mice ($n = 16$) and wild-type littermates ($n = 13$) with 5% reduction in the knock-in and P value between genotypes of 0.00006 (unpaired two-tailed t-test). **c**, T308A knock-in mice ($n = 16$) and wild-type littermates ($n = 13$) were scored for the presence of a hindlimb clasp. P value was 0.00005 (two-proportion Z-test). **d**, T308A knock-in mice ($n = 16$) and wild-type littermates ($n = 13$) were placed on an accelerating rotarod, and latency to fall was measured with a P value between genotypes of 0.02 (two-tailed t-test). **e**, T308A knock-in mice ($n = 17$) and wild-type littermates ($n = 15$) were injected with 40 mg kg^{-1} PTZ and latency to onset of generalized tonic-clonic seizures was measured. P value was 0.029 (two-sample Kolmogorov–Smirnov test). Error bars indicate s.e.m.

METHODS SUMMARY

Phosphotryptic mapping was performed on MeCP2 derived from neurons that were pre-treated with ^{32}P-orthophosphate and membrane-depolarized with KCl. MeCP2 T308A knock-in mice were generated as described previously[14].

Full Methods and any associated references are available in the online version of the paper.

Received 25 July 2012; accepted 4 June 2013.
Published online 16 June 2013.

1. Nan, X., Campoy, F. J. & Bird, A. Mecp2 is a transcriptional repressor with abundant binding sites in genomic chromatin. *Cell* **88,** 471–481 (1997).
2. Nan, X. *et al.* Transcriptional repression by the methyl-Cpg-binding protein Mecp2 involves a histone deacetylase complex. *Nature* **393,** 386–389 (1998).
3. Skene, P. J. *et al.* Neuronal Mecp2 is expressed at near histone-octamer levels and globally alters the chromatin state. *Mol. Cell* **37,** 457–468 (2010).
4. Amir, R. E. *et al.* Rett syndrome is caused by mutations in X-linked Mecp2, encoding methyl-CpG-binding protein 2. *Nature Genet.* **23,** 185–188 (1999).
5. Chahrour, M. *et al.* Mecp2, a key contributor to neurological disease, activates and represses transcription. *Science* **320,** 1224–1229 (2008).
6. Ballestar, E., Yusufzai, T. M. & Wolffe, A. P. Effects of Rett syndrome mutations of the methyl-Cpg binding domain of the transcriptional repressor Mecp2 on selectivity for association with methylated DNA. *Biochemistry* **39,** 7100–7106 (2000).
7. Ho, K. L. *et al.* Mecp2 binding to DNA depends upon hydration at methyl-Cpg. *Mol. Cell* **29,** 525–531 (2008).
8. Lyst, M. J. *et al.* Rett syndrome mutations abolish the interaction of MeCP2 with the NCoR/SMRT co-repressor. *Nature Neurosci.* http://dx.doi.org/10.1038/nn.3434 (16 June 2013).
9. Chen, W. G. *et al.* Derepression of Bdnf transcription involves calcium-dependent phosphorylation of Mecp2. *Science* **302,** 885–889 (2003).

10. Zhou, Z. *et al.* Brain-specific phosphorylation of Mecp2 regulates activity-dependent Bdnf transcription, dendritic growth, and spine maturation. *Neuron* **52,** 255–269 (2006).
11. Tao, J. *et al.* Phosphorylation of Mecp2 at serine 80 regulates its chromatin association and neurological function. *Proc. Natl Acad. Sci. USA* **106,** 4882–4887 (2009).
12. Li, H., Zhong, X., Chau, K. F., Williams, E. C. & Chang, Q. Loss of activity-induced phosphorylation of Mecp2 enhances synaptogenesis, Ltp and spatial memory. *Nature Neurosci.* **14,** 1001–1008 (2011).
13. Ebert, D. H. & Greenberg, M. E. Activity-dependent neuronal signalling and autism spectrum disorder. *Nature* **493,** 327–337 (2013).
14. Cohen, S. *et al.* Genome-wide activity-dependent Mecp2 phosphorylation regulates nervous system development and function. *Neuron* **72,** 72–85 (2011).
15. Kokura, K. *et al.* The Ski protein family is required for Mecp2-mediated transcriptional repression. *J. Biol. Chem.* **276,** 34115–34121 (2001).
16. Li, J. *et al.* Both corepressor proteins Smrt and N-Cor exist in large protein complexes containing Hdac3. *EMBO J.* **19,** 4342–4350 (2000).
17. Perissi, V., Jepsen, K., Glass, C. K. & Rosenfeld, M. G. Deconstructing repression: evolving models of co-repressor action. *Nature Rev. Genet.* **11,** 109–123 (2010).
18. Lin, Y. *et al.* Activity-dependent regulation of inhibitory synapse development by Npas4. *Nature* **455,** 1198–1204 (2008).
19. Dani, V. S. *et al.* Reduced cortical activity due to a shift in the balance between excitation and inhibition in a mouse model of Rett syndrome. *Proc. Natl Acad. Sci. USA* **102,** 12560–12565 (2005).
20. Wayman, G. A., Lee, Y. S., Tokumitsu, H., Silva, A. J. & Soderling, T. R. Calmodulin-kinases: modulators of neuronal development and plasticity. *Neuron* **59,** 914–931 (2008).
21. Hong, E. J., McCord, A. E. & Greenberg, M. E. A biological function for the neuronal activity-dependent component of Bdnf transcription in the development of cortical inhibition. *Neuron* **60,** 610–624 (2008).
22. Collins, A. L. *et al.* Mild overexpression of Mecp2 causes a progressive neurological disorder in mice. *Hum. Mol. Genet.* **13,** 2679–2689 (2004).
23. Ramocki, M. B., Tavyev, Y. J. & Peters, S. U. The Mecp2 duplication syndrome. *Am. J. Med. Genet. A.* **152A,** 1079–1088 (2010).

Supplementary Information is available in the online version of the paper.

Acknowledgements This work was supported by NIH grant RO1NS048276 and the Rett Syndrome Research Trust to M.E.G. D.H.E was supported by NIH grant K08MH90306, the Dupont–Warren Fellowship in the Department of Psychiatry at Harvard Medical School, and the Nancy Lurie Marks Fellowship in Autism at Harvard Medical School. H.W.G. was supported by Damon Runyon Cancer Research Foundation Grant DRG-2048-10. The Mouse Gene Manipulation Facility of the Boston Children's Hospital Intellectual and Developmental Disabilities Research Center (IDDRC), funded by NIH grant P30-HD 18655, assisted in generation of the knock-in mice. We thank members of the Greenberg laboratory, particularly C. Mandel-Brehm and E. Griffith, and also G. Mandel and R. S. Greenberg for helpful discussions.

Author Contributions D.H.E. and M.E.G. conceived and designed the experiments and wrote the manuscript. D.H.E. performed or directed all the experiments in the manuscript. D.H.E., N.D.R. and N.R.K. generated and characterized the MeCP2 T308A knock-in and R306C knock-in mice and characterized activity-dependent phosphorylation of MeCP2. H.W.G. performed the ChIP analysis, and H.W.G. and S.C. performed experiments investigating activity-dependent phosphorylation of MeCP2 that informed this study. D.H.E., L.S.H. and N.D.R. developed the phospho-site-specific antibodies, and A.J.N. assisted in early work with these antibodies during summer rotations. M.J.L., R.E. and A.P.B. discovered that the RTT missense mutation R306C disrupted both the interaction with NCoR and MeCP2's ability to provide transcription repression using the luciferase reporter assay. All authors reviewed the manuscript.

Author Information Reprints and permissions information is available at www.nature.com/reprints. The authors declare no competing financial interests. Readers are welcome to comment on the online version of the paper. Correspondence and requests for materials should be addressed to M.E.G. (michael_greenberg@hms.harvard.edu).

METHODS

Gene nomenclature. To maintain consistency of nomenclature with past descriptions of phosphorylation of MeCP2 S421 and RTT missense mutations, the S86, S274, T308 and S421 nomenclature refers to the mouse MeCP2 isoform 2 (MeCP2_e2; NCBI reference sequence NP_034918). S86, S274, T308 and S421 in mouse MeCP2 isoform 2 correspond to S103, S291, T325 and S438, respectively, in the mouse MeCP2 isoform 1 (MeCP2_e1; NCBI reference sequence NP_001075448), correspond to S86, S274, T308 and S423 in the human MeCP2 isoform 1 (NCBI reference sequence NP_004983), and correspond to S98, S286, T320 and S435 in human MeCP2 isoform 2 (NCB1 reference sequence NP_001104262). Alternative splicing generates the two MeCP2 isoforms, which are distinguished by distinct N-terminal sequences.

Neuronal cell culture. Primary dissociated cortical neuron cultures were derived from cortices of mice at embryonic day 16 (E16), as previously described[24], and cultured for varying days *in vitro* (DIV), allowing for neuronal maturation and synapse development in culture. Cortical cultures were maintained in neurobasal medium with B27 supplement (Invitrogen), 1 mM L-glutamine, and 100 U ml^{-1} penicillin/streptomycin. Cells were plated at 1–2 $\times 10^6$ on 6-well dishes, 10×10^6 on 10-cm dishes, and 30×10^6 on 15-cm dishes that had been pre-treated with polyornithine.

Phosphotryptic mapping of MeCP2. Dissociated E16 mouse cortical neurons at 6 DIV were treated overnight with 1 μM tetrodotoxin and 100 μM APV (Tocris Bioscience) to reduce endogenous neuronal activity in the culture. At 7 DIV, cortical neuron cultures, in 10-cm dishes, were labelled with 2.5 mCi of ^{32}P-orthophosphate (Perkin Elmer) in phosphate-free neurobasal medium for 5 h. Neurons were then left untreated or exposed to 55 mM KCl by addition of 0.5 volumes of depolarization buffer (170 mM KCl, 2 mM $CaCl_2$, 1 mM $MgCl_2$ and 10 mM HEPES, pH 7.5) for 90 min, to induce membrane depolarization and robustly model neuronal activity. Neurons were washed once in PBS, lysed in TTN lysis buffer (30 mM Tris, pH 7.5, 1 M NaCl, 3% Triton X-100, 5 mM EDTA, 10 mM β-glycerolphosphate, 10 mM NaF, 2 mM Na_3VO_4, and 1× complete EDTA-free protease inhibitor cocktail (Roche)), and sheared with a 22-gauge needle. Insoluble material was pelleted at 17,000*g* and removed. Lysates were diluted with equal volumes of H_2O to reduce NaCl concentration to 500 mM. Lysates were immunoprecipitated with an anti-total MeCP2 antibody (antibody to the C terminus of MeCP2 that was generated in-house as described previously[10]) bound to protein A sepharose beads for 2 h while rotating at 4 °C. Immunoprecipitates was washed four times in TTN buffer (diluted to 500 mM NaCl and 1.5% Triton X-100) and resolved by SDS–PAGE. The dried gel was exposed to autoradiography. Phosphotryptic mapping of MeCP2 followed the procedure detailed in ref. 25. The MeCP2 band was excised from the gel and digested with trypsin (TPCK-treated, Worthington). The tryptic phosphopeptides were separated in two-dimensions by thin-layer electrophoresis, using pH 1.9 electrophoresis buffer (2.5% formic acid (88% w/v) and 7.8% glacial acetic acid), for 30 min at 1,000 V and by thin-layer chromatography, using the phosphochromatography buffer (37.5% *n*-butanol, 25% pyridine, and 7.5% glacial acetic acid), on glass-backed TLC plates (20 × 20 cm, 100 μM cellulose, EM Science). The phosphotryptic maps were visualized by autoradiography. Experiments shown were repeated greater than three times using biological replicates from dissection of independent litters.

***In vitro* kinase assays.** MeCP2 fragments were generated by calcium phosphate transfection of HEK 293T cells with constructs expressing Flag-tagged N-terminal MeCP2 variants from amino acid 1 to 193 or C-terminal MeCP2 variants from amino acid 173 to 484. Missense mutations at putative sites of phosphorylation were generated by site-directed mutagenesis using Quickchange (Stratagene) and fully sequenced through the entire subcloned segment. HEK 293T cells were transfected by calcium phosphate. Forty-eight hours after transfection, the exogenous MeCP2 variants were collected in lysis buffer (50 mM Tris, pH 7.5, 500 mM NaCl, 2.5% Triton X-100, 2 mM EDTA, 10 mM NaF, 2 mM Na_3VO_4, 1 mM DTT, and 1× complete EDTA-free protease inhibitor cocktail (Roche)), immunoprecipitated with anti-Flag antibodies (M2, Sigma), and eluted from the beads with Flag peptides at 150 ng μl^{-1} concentration. The purified MeCP2 variants were phosphorylated using *in vitro* kinase assays. For *in vitro* kinase assays with CaMKIV, C-terminal fragments of MeCP2 were incubated in a reaction mixture with 40 mM Tris, pH 7.5, 10 mM $MgCl_2$, 0.5 mM $CaCl_2$, 1 mM DTT, 50 μg ml^{-1} calmodulin (Calbiochem), purified CaMKIV (recombinant, *Escherichia coli*, Life Technologies), 0.1 mM cold ATP, and 5 μCi (0.033 μM) [γ-^{32}P]ATP (Perkin Elmer) in a 25 μl reaction for 10–30 min at 30 °C. For *in vitro* kinase assays with PKA, purified MeCP2 variants were incubated in a reaction mixture with 40 mM Tris, pH 7.5, 10 mM $MgCl_2$, 1 mM DTT, PKA (catalytic subunit, mouse, recombinant, *E. coli*, Calbiochem), 0.1 mM cold ATP and 5 μCi (0.033 μM) [γ-^{32}P]ATP in a 25 μl reaction for 10–30 min at 30 °C.

Generation of anti-MeCP2 phospho-site-specific antibodies. The polyclonal antibody that specifically recognizes S86-phosphorylated MeCP2 was generated by injecting New Zealand White rabbits (Covance Research Products) with the peptide KQRR(p**S**)IIRDRGPM-C (Tufts Synthesis Facility) conjugated to KLH. The antiserum was affinity-purified by incubation with a column that was conjugated with phosphorylated-S86 MeCP2 peptide, and the affinity-purified antibody was eluted. This eluate was then incubated with a column conjugated with unphosphorylated-S86 MeCP2 peptide, and the affinity-purified anti-MeCP2 pS86 antibody was collected in the flow-through. The polyclonal antibody that specifically recognizes S274-phosphorylated MeCP2 was generated by injecting rabbits with the peptide RKPG(p**S**)VVAAAAAEAKKK-C conjugated to KLH. The antibody was affinity purified similar to the purification of the anti-MeCP2 pS86 antibodies. The polyclonal antibody that specifically recognizes T308-phosphorylated MeCP2 was generated by injecting rabbits with the peptide C-TVLPIKKRK(p**T**)RE conjugated to KLH. The antibody was purified over a column conjugated with MeCP2 T308 peptide, and the affinity-purified anti-MeCP2 pT308 was eluted. The generation of the polyclonal rabbit antibody that specifically recognizes S421-phosphorylated MeCP2 and the polyclonal antibody that recognizes total MeCP2 irrespective of phosphorylation status were previously described[10].

Stimulation of MeCP2 phosphorylation in cell culture and *in vivo*. Cortical neuron cultures (E16 + 7 DIV) were membrane depolarized with 55 mM KCl by addition of 0.5 volumes of depolarization buffer (170 mM KCl, 2 mM $CaCl_2$, 1 mM $MgCl_2$ and 10 mM HEPES, pH 7.5). Alternatively, cultures were treated with 20 μM forskolin (Calbiochem) or 50 ng ml^{-1} BDNF (Peprotech) for 30 min or 1 h. For bicuculline experiments, E16 + 14 DIV cortical neuron cultures were treated with 20 μM bicuculline (Sigma) for 30–120 min. For western blot analysis, cells were lysed in boiling sample buffer to preserve endogenous phosphorylation events and prevent spurious phosphorylation events after cell lysis. Lysates were boiled for 10 min, passed through Wizard Minicolumns (Promega) to remove larger molecules and insoluble material, and resolved by 8% SDS–PAGE gels, normalized by cell number. Western blotting was performed with antibodies specific to MeCP2 phosphorylation sites (generated in our laboratory as described above) or specific to total MeCP2 irrespective of phosphorylation status (Men-8, Sigma) or β-actin (ab8226, Abcam), all at 1:1,000 dilutions. Western blotting was completed with HRP-conjugated secondary antibodies and enhanced chemiluminescence. Seizures were induced in adult C57B/6 male mice, or in MeCP2 knockout male mice (MeCP2$^{tm1.1Bird}$ line acquired from Jackson laboratories), 8–10 weeks of age, by intraperitoneal injection of kainic acid at a dosage of 25 mg kg^{-1}. Ninety minutes after injection, forebrains were collected and lysed in boiling sample buffer to preserve phosphorylation sites, and lysates were analysed by western blotting as described previously. Experiments shown were replicated at least three times using biological replicates from dissection of independent animals with the same results.

Endogenous co-immunoprecipitation. Eight-week-old C57B/J mice were left untreated or seizures were induced by intraperitoneal injection of kainic acid at a dosage of 25 mg kg^{-1}. Two hours after injection, forebrains were isolated and lysed in NP-40 lysis buffer (10 mM HEPES, pH 7.9, 3 mM $MgCl_2$, 10 mM KCl, 10 mM NaF, 1 mM Na_3VO_4, 0.5 mM DTT, 0.5% NP-40, 1× complete EDTA-free protease inhibitor cocktail (Roche)), dounced 15× with a tight pestle, and pelleted at 1,000*g*. Lysates were diluted 1:1 with benzonase buffer (10 mM HEPES, pH 7.9, 3 mM $MgCl_2$, 280 mM NaCl, 0.2 mM EDTA, 10 mM NaF, 1 mM Na_3VO_4, 0.5 mM DTT, 0.5% NP-40, and 1× complete EDTA-free protease inhibitor cocktail (Roche)) and digested with 250 units of the permissive nuclease benzonase (Novagen) for 1 h rotating at 4 °C to release MeCP2 and its protein binding partners from the genome. Digested lysates were pelleted at 17,000*g* for 20 min at 4 °C and immunoprecipitated with anti-total MeCP2 antibodies (raised in house as in ref. 10), in either the presence of 150 mM NaCl or 250 mM NaCl as indicated, for 2 h while rotating at 4 °C. The peptide-block control was immunoprecipitation of lysates with anti-total MeCP2 antibodies in the presence of the peptide to which the antibody was raised. Western blots of SDS–PAGE resolved immunoprecipitates are shown using anti-NCoR (PA1-844A, Pierce) and anti-MeCP2 antibodies (generated in-house).

Peptide pull-down assays. To investigate the impact of phosphorylation of MeCP2 T308 on binding to other proteins, we synthesized a peptide corresponding to MeCP2 amino acids 285–319 with biotin conjugated to the N terminus of the peptide (Tufts University Core Facility). This peptide (Biotin-KKAVKESSIR SVHETVLPIKKRK[**T**]RETVSIEVKEV) was left unphosphorylated or phosphorylated at the amino acid residue corresponding to T308 (the bold T in brackets). We synthesized additional variant peptides, including a variant in which the amino acid residue corresponding to R306 was synthesized as a cysteine (R306C) and variants in which the amino acid residue corresponding to T308 was synthesized as either an alanine, glutamic acid, or aspartic acid (T308A, T308D, or T308E). The biotin-conjugated peptides, from 0.1 to 5 μg, were bound to 40 μl Streptavidin MagneSphere Paramagnetic Particles (Promega) during a greater than 1 h rotation at 4 °C before incubation with neuronal cell lysates. Cortical neuron cultures (E16 + 7 DIV) were scraped in PBS, lysed in lysis buffer (10 mM HEPES, pH 7.8, 500 mM NaCl, 1% Triton X-100, 10 mM NaF, 1 mM Na_3VO_4, 5 mM EDTA, 0.5 mM DTT,

and 1× complete EDTA-free protease inhibitor cocktail (Roche)), sheared with a 22-gauge needle, and pelleted at 17,000*g* for 20 min at 4 °C. Lysates were diluted 1:2 with dilution buffer (10 mM HEPES, pH 7.8, 0.5% Triton X-100, 10 mM NaF, 1 mM Na_3VO_4, 5 mM EDTA, 0.5 mM DTT, and 1× complete EDTA-free protease inhibitor cocktail (Roche)) to lead to a final NaCl concentration in the lysate of approximately 167 mM. Neuronal lysates were incubated with biotin-conjugated beads bound to streptavidin particles, rotating at 4 °C for 16 h. The peptide pull-down was washed four times with wash buffer (10 mM HEPES pH 7.8, 150 mM NaCl, 0.5% Triton X-100, 10 mM NaF, 1 mM Na_3VO_4, 5 mM EDTA, and 0.5 mM DTT) and boiled in 1.2× sample buffer for 10 min. The peptide pull-downs were resolved by SDS–PAGE, 5% gel for NCoR and 10% gels for the other proteins. Western blotting was performed with antibodies specific to NCoR (PA1-844A, Pierce), HDAC3 (H3034, Sigma), TBL1 (H-367, Santa Cruz), TBLR1 (ab13799, Abcam), GPS2 (H-225, Santa Cruz), Coronin 2A (M-105, Santa Cruz) and SIN3A (N-19, Santa Cruz).

Transcription repression domain assay. Cortical neurons (2.5×10^5) were plated into wells of 24-well plate and neurons (E16 + 5 DIV) were transfected by calcium phosphate procedure[26] with multiple plasmids. All cells were transfected with a plasmid encoding the firefly luciferase with constitutively active TK-promoter and 5× UAS binding sites for GAL4 upstream of the promoter and with a plasmid encoding renilla luciferase, to normalize transfection between samples[1,8]. In the different conditions, cells were transfected with plasmids encoding fusion proteins between GAL4 and MeCP2 variants. The GAL4–MeCP2 fusion proteins extend from MeCP2 amino acid 201 to 484 and are missing the DNA-binding domain from MeCP2. The GAL4–MeCP2 fusion proteins are brought to the reporter plasmid by interaction between the UAS sequence and GAL4 subunit of the fusion protein. We generated missense mutations at amino acid residue corresponding to MeCP2 T308 to A, D, and E by site-directed mutagenesis using Quikchange (Stratagene). Neurons were transfected with 0.4 μg firefly luciferase plasmid, 0.08 μg renilla luciferase plasmid, 0.03 μg GAL4–MeCP2 variant plasmid, and PCS2 filler plasmid to 1 μg total per well. At 7 DIV, cells were collected for measurement of firefly and renilla luciferase, using Dual-Luciferase Reporter Assay (Promega). The ratio of firefly to renilla luciferase was calculated for each well. Shown is average of ratio of firefly to renilla luciferase of three biological replicates with standard deviation, normalized to condition without any GAL4–MeCP2 variant transfected (labelled 'none' in Fig. 2d). The experiment was repeated independently three times from dissections of independent litters with the same results.

MeCP2 R306C knock-in mice. MeCP2 R306C knock-in mice were generated in the Greenberg laboratory as previously described[14], and the homologous recombination was confirmed by sequencing and Southern blot analysis. Eight-week-old MeCP2 R306C knock-in male mice and wild-type littermates were injected with 25 mg kg^{-1} of kainic acid to induce seizures. After one hour, forebrains were dissected and lysed in boiling sample buffer and with shearing from a Polytron. Lysates were resolved for western blot analysis with the anti-MeCP2 pT308, anti-MeCP2 pS421, and anti-total MeCP2 antibodies. The experiment was repeated with five biological replicates from independent animals with the same results.

MeCP2 T308A knock-in mice. MeCP2 T308A knock-in mice were generated using the same approach as previously described[14], and the homologous recombination was confirmed by sequencing and Southern blot analysis. The targeting construct contained the mutation, ACC to GCC, for the codon corresponding to amino acid 308. Given that MeCP2 is on the X chromosome, all experiments used male knock-in or wild-type littermates.

To determine whether MeCP2 T308A knock-in mice could be phosphorylated at T308, 10-week-old mice were injected with 25 mg kg^{-1} of kainic acid, or left untreated, and, after one hour, forebrain lysates were resolved for western blot analysis with indicated antibodies. For MeCP2 protein levels, brains were dissected from MeCP2 T308A knock-in mice and wild-type littermates. Brains were lysed in boiling sample buffer, sheared with a Polytron, and resolved for western blot analysis.

For MeCP2 ChIP, forebrains of 11-week-old mice were dissected on ice, and crosslinking and nuclear preps were performed as described[14]. To fragment chromatin, SDS was added to 0.3% final concentration, and samples were sonicated using a Covaris S2 sonicator (12 min, 5% duty cycle, power level 4, 200 cycles per burst). Similar fragmentation was confirmed for all samples by gel electrophoresis, with ~80% of the DNA appearing as a smear from approximately 100–500 bp in length. For immunoprecipitation, rabbit polyclonal antisera recognizing total MeCP2[9] were used as previously described[14] except that ChIP buffer containing SDS instead of NaDOC was used for the sample during the immunoprecipitation (10 mM Tris pH 8.0, 0.1% SDS, 1% Triton X-100, 150 mM NaCl, 1 mM EDTA, 0.3 mM EGTA, 1× Roche complete EDTA-free protease inhibitors, 10 mM β-glycerolphosphate, 10 mM NaF). After overnight incubation the supernatant was discarded and beads were washed at 4 °C with the following washes: 2 times with low salt wash buffer (0.1% SDS, 20 mM Tris pH 8.0, 1% Triton X-100, 150mM NaCl, 2 mM EDTA), 2 times with high salt wash buffer (0.1% SDS, 20 mM Tris pH 8.0, 1% Triton X-100, 500 mM NaCl, 2 mM EDTA), 2 times with LiCl wash buffer (0.1% NaDOC, 10 mM Tris pH 8.0, 1% NP40, 250 mM LiCl, 1 mM EDTA), once with TE. DNA was eluted by incubation for 30 min at 65 °C in TE containing 1% SDS. Input and immunoprecipitated DNA were decrosslinked by incubating for 12–16 h at 65 °C, treated with RNase (20 μM RNase A at 37 °C for 0.5–1 h) and proteinase K (280 μM at 55 °C for 2 h), phenol/chloroform extracted twice, chloroform extracted once, and DNA was isolated using a Qiagen PCR purification column (Qiagen).

Quantitative PCR analysis was carried out using the StepOnePlus qPCR system and Power SYBR Green mix (Life technologies). The 'fraction of input' value for each amplicon (primers listed below) was determined by comparing the average threshold cycle of the immunoprecipitated DNA to a standard curve generated using serial dilutions of the input DNA and interpolating the 'fraction of input' value for the sample. All sites of amplification showed significant >10 fold increased signal compared to MeCP2 ChIP done from MeCP2 knockout mice. Primers used for ChIP-qPCR, identical to those used previously[14], were *Bdnf* upstream, GGCCAAGGTGAATTGGGTAT, TGATGGCAGCAATGTTTCTC, −29 kb to TSS; *Actb* TSS, AGTGTCTACACCGCGGGAAT, CTGGCACAGCCA ACTTTACG, 236 bp to TSS; *Npas4* TSS, AGGGACCCAGGTTTTCCAT, GGGCTTCAGACCACCCTAAT, −313 bp to TSS; and major satellite, GGCG AGAAAACTGAAAATCACG, AGGTCCTTCAGTGTGCATTTC.

For gene expression analysis in the stimulated visual cortex, MeCP2 T308A knock-in male mice and wild-type male littermates were placed in the dark at 6 weeks of age. Two weeks later, mice were kept in the dark or exposed to light for 6 h. Visual cortices were dissected. RNA was purified by TRIzol (Life Technologies) extraction, RNeasy Mini kit (Qiagen) with on-column DNase digestion (RNase-Free DNase Set, Qiagen). From 1.0 μg RNA, cDNA was generated using random primers (High Capacity cDNA Reverse Transcription Kit, Applied Biosystems). Quantitative PCR (qPCR) was performed using LightCycler 480 Real-Time PCR instrument (Roche) with LightCycler 480 SYBR Green 1 master mix (Roche). The primers used for *Npas4* were GCTATACTCAGAAGGTCCA GAAGGC, TCAGAGAATGAGGGTAGCACAGC; *Bdnf*, GATGCCGCAAA CATGTCTATGA, TAATACTGTCACACACGCTCAGCTC; *Arc*, TACCGTTA GCCCCTATGCCATC, TGATATTGCTGAGCCTCAACTG; β-tubulin, CGAC AATGAAGCCCTCTACGAC, ATGGTGGCAGACACAAGGTGGTTG.

Values at each time point were normalized to β-tubulin. To illustrate the induced gene expression on one graph, values were divided by average of the wild-type 6-h time point for each gene tested. Sample size was chosen to detect magnitude of gene expression changes consistent with magnitude of gene expression changes reported in MeCP2 knockout mice. The *P* values were calculated by unpaired two-tailed Student's *t*-test.

In addition, dissociated E16.5 cortical neuron cultures were generated from MeCP2 T308A knock-in males and wild-type littermates and 7.5×10^5 cells were plated per well of a 6-well dish. Cultures were fed at 7 DIV with 30% fresh NB media. At 10 DIV, cultures were treated with AP5 and TTX to silence activity in the culture for 2 h before starting the 6-h membrane depolarization time point. Cultures were membrane depolarized with 55 mM KCl for 1 h, 3 h, or 6 h or left untreated. Cells were lysed in TRIzol, and RNA purified and cDNA generated as above. Three wells per condition in an experiment were combined to make one sample. To show fold-induction of gene expression over the time course, values at each time point were divided by the value at 0 h. Three independent days of dissection and experiments (biological replicates) were averaged for the qPCR experiments shown. *P* values were calculated by two-way repeated measures ANOVA and by two-tailed Student's *t*-test at specific time points, pairing wild-type and knock-in neurons derived from the same litters, combined on the day of dissection, for the three independent days of dissection and culturing of neurons.

MeCP2 T308A knock-in males ($n = 16$) and wild-type littermate males ($n = 13$) were weighed at 14–16 weeks of age. Whole brains were then dissected and weighed. A second independent cohort of MeCP2 T308A knock-in mice ($n = 9$) and wild-type littermates ($n = 9$) had identical findings with the same magnitude of difference between genotypes. *P* values were calculated by two-tailed, unpaired student's *t*-test.

To determine the presence of a hindlimb clasp, MeCP2 T308A knock-in male mice ($n = 16$) and wild-type male mice ($n = 13$), at 11–13 weeks of age, were lifted by their tails, to a height one foot off the table. The presence of a hindlimb clasp was defined as pulling in one or both of the hindlimbs fully towards the body for at least 2 s. Each mouse was scored, blinded to genotype, for the presence of a hindlimb clasp during three rounds of two-minute observation, with 5 min between each round. A second independent cohort of MeCP2 T308A knock-in mice ($n = 9$) and wild-type littermates ($n = 9$) had identical findings. *P* value, calculated by two-proportion *Z*-test, was 0.00005.

MeCP2 T308A knock-in mice ($n = 16$) and wild-type littermates ($n = 13$) were tested on an accelerating rotarod (Economex, Columbus Instruments) at 13–15 weeks of age. Animals were brought in 30 min before testing for habituation. Each animal was placed on an accelerating rotarod set to 4.0–40 r.p.m. over a period of 5 min. A fall was called either when an animal fell off the rod or rotated twice around without recovery. Littermates were given two to four trials with an hour of rest in between, and an average latency to fall was calculated for each animal. The statistical test used to compare fall latency across the two genotypes was a two-tailed, unpaired Student's *t*-test.

To evaluate seizure threshold, MeCP2 T308A knock-in mice ($n = 17$) and wild-type littermates ($n = 15$) were injected with pentylenetetrazol (PTZ), a GABA receptor antagonist, at 14 –16 weeks of age. Mice were habituated to the room for 20 min and weighed. Mice were injected intraperitoneally with 40 mg kg^{-1} of PTZ (Sigma Aldrich). Mice were scored for time to onset of a generalized tonic-clonic seizure for 30 min following injection of PTZ.

The behavioural characterization of the T308A knock-in mice in this manuscript was performed at fifth generation backcross to C57B/6 from the 129J ES cell line used to generate the mice. Experiments involving mice were performed blinded to genotype. Sample size for behavioural experiments, of 13–17 male mice per genotype, was chosen to mitigate against genetic background variance. Only litters with at least one male of each genotype, T308A knock-in and wild type, were used for analysis. All mice in the behavioural experiments had the same tests and experiences; there was no randomization used. Mice were tested in the following order: hindlimb clasp, rotarod and PTZ-induction of seizures. There was at least one week between tests. The independent two-tailed *t*-tests used met the test criteria in that the samples were independent, data in each sample were independent, and all population values appear normally distributed (unimodal histogram and symmetric). For the PTZ-induced seizures, a two-sample Kolmogorov–Smirnov (KS2) test was used to determine whether two one-dimensional probability distributions differ. Variances across genotypes for all tests appear homoscedastic, as variances of s.d. are similar. All animal experiments were in compliance with ethical regulations and were approved by the Harvard Medical Area Standing Committee on Animals (HMA IACUC).

24. Xia, Z., Dudek, H., Miranti, C. K. & Greenberg, M. E. Calcium influx via the NMDA receptor induces immediate early gene transcription by a MAP kinase/ERK-dependent mechanism. *J. Neurosci.* **16,** 5425–5436 (1996).
25. Meisenhelder, J., Hunter, T. & van der Geer, P. Phosphopeptide mapping and identification of phosphorylation sites. *Curr. Protoc. Mol. Biol.* Ch. 18, Unit 18 19 (2001).
26. Dudek, H., Ghosh, A. & Greenberg, M. E. Calcium phosphate transfection of DNA into neurons in primary culture. *Curr. Protoc. Neurosci.* Ch. 3, Unit 3 11 (2001).